PROJECT PLAN

Introduction

With its Precambrian center surrounded by progressively younger geological provinces (Fig. 1), the North American continent is, in many ways, an ideal region to investigate timely geophysical questions such as the relationship of geological age to variations in the thickness of the continental lithosphere, the nature of the lithosphere-asthenosphere boundary (LAB), or the relationship of upper-mantle anisotropy to present day flow and/or past tectonic events. The permanent Backbone Network (BN) component of USArray, complemented by the Transportable Array (TA), will provide an unprecedented density of recordings to address these questions.

In recent work, we have sought to study continental scale structure in two rather different manners. At Berkeley, we have developed the capability to invert three component long period seismograms to construct regional tomographic models of the upper mantle which include both radial and azimuthal anisotropy and can incorporate other constraints, such as SKS splitting data, and applied it to the North American continent. Our results have confirmed the presence of lateral variations in lithospheric and asthenospheric structure correlated with tectonic features, and of anisotropy in the asthenosphere. However, this model is laterally and vertically smooth, and the approach taken so far does not allow the detection and precise mapping of laterally varying horizons such as the LAB, and other deeper or shallower boundaries.

On the other hand, at Brown, we have developed methods to locally detect and characterize scattering horizons under individual stations, using teleseismic S to P (Sp) and P to S (Ps) converted phases. We have applied this to permanent broadband stations in the eastern US, showing the presence of a westward dipping discontinuity at depths of ~90 km that we identify as the LAB. In addition, the scattered waves provide tighter vertical resolution of the velocity gradient at this boundary than is possible with surface waves, indicating a 5-10% drop in shear-wave velocity over less than 11 km (*Rychert et al.*, 2005, 2006). However, although this approach gives us high resolution locally, it provides constraints only where there are stations. Moreover, when determining the depth of the detected discontinuities there are trade-offs with volumetric 3D structure above and below the discontinuity.

We propose to combine and merge these two complementary sets of tools, in order to develop the capability of mapping the 3D anisotropic structure of the upper mantle at the continental scale with high resolution both in the lateral and vertical directions.

Science Targets

The geology and tectonics of the North American continent divide its land-mass into two distinct provinces: the tectonically active western region and the stable central and eastern shields, with the boundary between them coinciding almost perfectly with the Rocky Mountain Front (Fig. 1). In western North America, eastward flat subduction of the oceanic Farallon lithosphere (75-40 Ma) is thought to be responsible for the Laramide orogeny, while about 40 Ma ago, the slab steepened and was gradually replaced by a transform system, giving rise to a growing slab window. As a consequence, the base of the crust over a vast region west of the Rockies was exposed to upwelling hot asthenosphere, contributing to additional uplift as well as crustal extension and magmatism in the Basin and Range (e.g. *Dickinson and Snyder*, 1979; *Bird*, 1984, 1988; *Severinghaus and Atwater*, 1990; *Humphreys et al.*, 2003). Currently tectonic activity is observed throughout the western part of the continent, and manifests itself in a wide variety of phenomena and deformation mechanisms. In fact, western North America is characterized by a complex plate boundary featuring most deformation styles possibly present at such margins: subduction of the Pacific Plate in the north and of the young Juan de Fuca plate offshore the western US-Canadian border, strike-slip along the Queen Charlotte-Fairweather system in Canada and along the San Andreas fault in California, extension in Baja California. In addition to recorded seismicity, there is evidence for recent tectonic activity such as, for example, Yellowstone volcanism and Holocene volcanism documented throughout the Cascadian Range, a region still experiencing ongoing continental arc volcanism.

Figure 1: Geological Provinces of North America. Green: Precambrian; Pink: Platform cover; brown: Paleozoic; blue: Mesozoic-tertiary. From *Bally et al.* (1989).

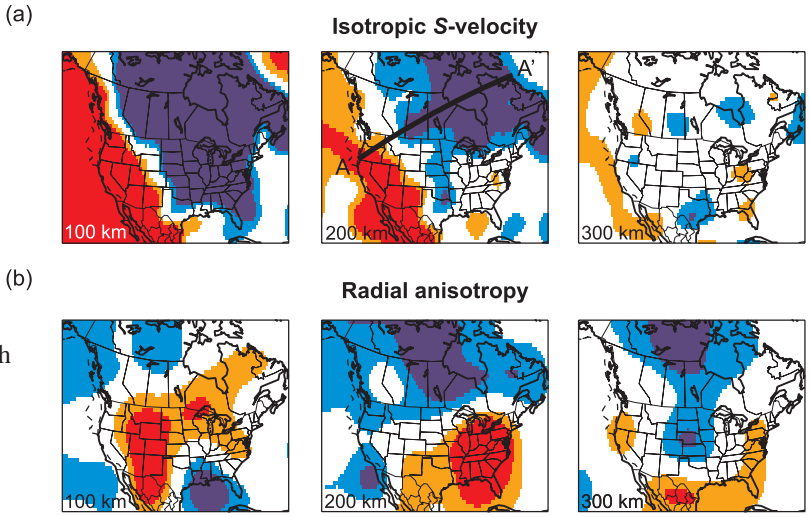

Figure 2. Radially anisotropic model of the north American upper mantle. (a) Isotropic S velocity at depths of 100, 200 and 300 km. (b) Radial anisotropy at the same depths, referred to the PREM model. Note that to obtain the total anisotropy at a depth of 100 km, PREM anisotropy of about +4% in ξ needs to be added. (c) Depth cross-sections through the profile AA' indicated in the top middle panel. While fast velocities wane out at depths >250 km, radial anisotropy persists to at least 400 km. From *Marone et al.* (2006).

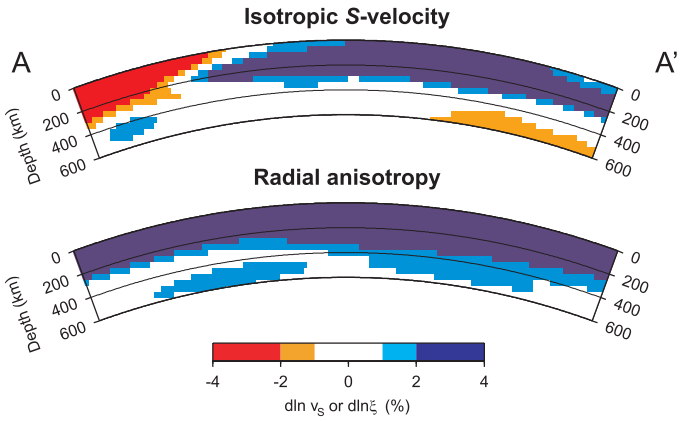

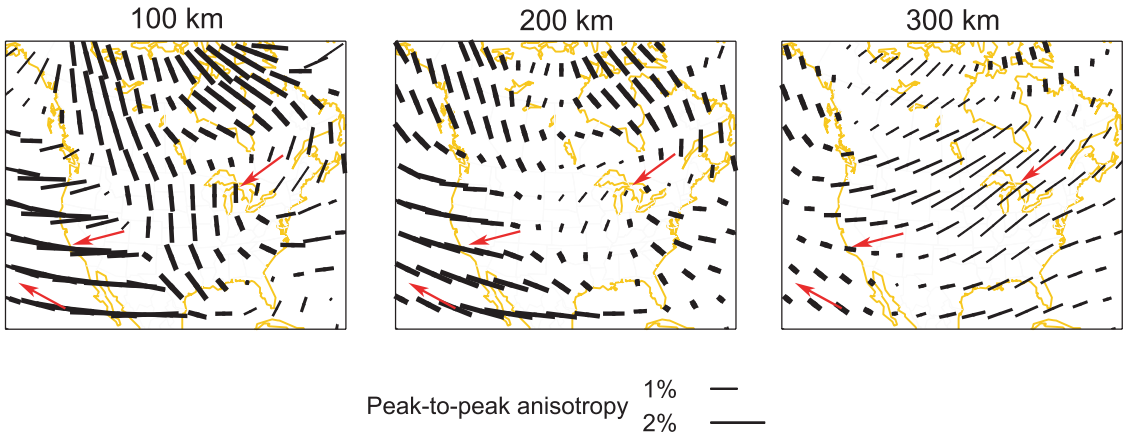

Figure 3. Distribution of azimuthal anisotropy in the north American upper mantle, obtained by inversion of long period waveform data (fundamental mode and overtone surface waves), with contraints from a compilation of SKS splitting measurements. The model is parametrized in spherical splines of "level 4", equivalent to spherical harmonics of degree ~24. Red arrows indicate the direction of absolute plate motions according to the Nuvel model.

The interior of the North American continent mainly consists of the Precambrian Continental Platform and the Canadian Shield, which have been stable since the Grenville orogeny and Midcontinent Rift formation at 1 Ga, with a few Archean cores (for example, the Superior and Slave provinces), which experienced their last deformation 2.5 Ga ago. In the eastern part of North America, following the Paleozoic collision of the proto-African and proto-North American plates (the Appalachian orogeny), the last major tectonic events to affect the lithosphere were Triassic and Jurassic rifting in the east related to the opening of the Atlantic Ocean and the subsequent passage of the lithosphere over the Great Meteor Hotspot plume ~100–120 Myr ago (e.g. *Hatcher*, 1989; *Heaman and Kjarsgaard*, 2000). However, the persistence of surface relief and evidence for Neogene uplift (*Pazzaglia and Brandon*, 1996; *Pazzaglia and Gardner*, 2000) pose unsolved questions for dynamic processes in the eastern US.

This tectonic diversity has led to a rich set of geological, tectonic and geodynamical models, and many of these could be better tested with higher resolution constraints on the local thickness and velocity structure of the continental lithosphere and asthenosphere, as well as deeper upper mantle structure. A better understanding of mantle lithospheric structure would help to explain observed differences in the style and degree of crustal deformation in almost any region, for example the transition from the Colorado Plateau to the Basin and Range (e.g. *Zandt et al*., 1995; *Humphreys et al*., 2003), and how they relate to asthenospheric flow and buoyancy. The proposed work will also address several broader themes:

How does the thickness of the North American lithosphere vary as a function of age? Do lithospheres of different ages exhibit distinct velocities that are diagnostic of compositional or thermal variations? How do these relate to global xenolith data indicating that progressively older cratonic lithospheres in general exhibit greater degrees of chemical depletion due to melting and cooler paleogeotherms (e.g. *Boyd*, 1989; *Rudnick et al*., 1998; *Poudjom Djomani et al*., 2001)? How does lithospheric anisotropy relate to the deformation histories of different tectonic provinces?

Does a continuous low-velocity layer (or asthenosphere) exist below the North American lithosphere? Does it contain significant lateral velocity variations and how might these reflect composition and temperature? How does asthenospheric anisotropy relate to the shape of the LAB? What are the implications of asthenospheric anisotropy for mantle flow and for lithosphere-asthenosphere coupling?

Is the LAB detectable everywhere, and how does the sharpness of the velocity gradient associated with it vary across the continent? Where can LAB gradients be explained by purely thermal models, and where do they require compositional differences (e.g. a more hydrated, less depleted asthenosphere) or the presence of partial melt in the asthenosphere? Can we detect the base of the asthenosphere and does it vary laterally?

How do deeper mantle interfaces – for example the 410 km discontinuity – vary laterally and what does that imply about mantle thermal state? Does 410 discontinuity topography shed light on the position of the subducted Farallon slab in the transition zone?

Previous studies

Global and regional tomography

Knowledge of the shear-wave anisotropic structure of the North American upper mantle results primarily from global and regional tomographic models and SKS splitting studies. Mapping of upper mantle radial and azimuthal anisotropy at the global scale has been achieved primarily using fundamental mode surface waves (e.g. *Tanimoto and Anderson*, 1984; *Montagner and Tanimoto*, 1991; *Ekström and Dziewonski*, 1998). Such studies have revealed the presence of significant radial anisotropy in the depth range 80-200 km under ocean basins, particularly in the Pacific, with $V_{SH} > V_{SV}$. Inclusion of overtones in the development of recent global tomographic models (e.g. *Gung et al., 2003*; *Panning and Romanowicz*, 2006) improves the resolution of anisotropy at depth. Such models have shown, in particular, that a zone of radial anisotropy with $V_{SH} > V_{SV}$ also exists under continental cratons such as the Canadian shield, but at greater depth (~200-400 km), suggesting that horizontal shear is present in the sub-lithospheric asthenosphere both under continents and oceans, at varying depths depending on the thickness of the lithosphere. A similar interpretation of global upper mantle anisotropy distribution has been suggested by *Plomerova et al*. (2002).

At the regional scale, most tomographic studies of North America have focused on the analysis of Rayleigh wave dispersion (*e.g. Alsina et al.*, 1996; *Godey et al.,* 2003), or waveform data in the framework of elastic isotropy (e.g. *Van der Lee and Nolet*, 1997; *Frederiksen et al.*, 2001; *Van der Lee*, 2002), with recent efforts to also map azimuthal anisotropy (*Li et al.*, 2003, 2005) or, using 3 component data, radial anisotropy (*Nettles and Dziewonski*, 2004). Azimuthal anisotropy in the North American upper mantle has been extensively studied using SKS splitting measurements (e.g. *Silver and Chan*, 1988; *Savage et al.*, 1990; *Vinnik et al.*, 1992; *Silver and Kaneshima*, 1993; *Bostock and Cassidy*, 1995; *Liu et al.,* 1995; *Özalaybey and Savage*, 1995; *Barruol et al.,* 1997; *Kay et al.,* 1999; *Levin et al.*, 1999; *Fouch et al.*, 2000; *Savage and Sheehan*, 2000). Models derived with this approach show, for instance, rapid variations of the fast axis direction of anisotropy in the western US and more slowly varying directions in the central and eastern US. However, such measurements do not provide any constraints on the depth of the anisotropic layer and strong tradeoffs between the strength of anisotropy and the thickness of the anisotropic layer exist. Because of these tradeoffs, shear-wave splitting analysis is not suitable, by itself, to test hypotheses regarding the depth and origin of the observed anisotropy. Nor can it definitively address questions about the relation of upper mantle anisotropy to present day asthenospheric flow and/or past tectonic events, even though detection of the presence of more than one layer of anisotropy is possible (e.g. *Savage and Silver*, 1993) as has been found in the Appalachians (*Levin et al.*, 1999). By comparing results from splitting measurements and surface wave azimuthal anisotropy, *Li et al.* (2003) infer the presence of anisotropy at depths greater than 200 km beneath eastern North America. Likewise, in a recent study of the eastern North American upper mantle, *Gaherty* (2004) combines constraints from surface waves and splitting measurements and suggests the presence of two layers of anisotropy, a lithospheric and an asthenospheric layer.

Recently, starting from a global mantle waveform tomography approach (e.g. *Li and Romanowicz*, 1995, 1996; *Mégnin and Romanowicz*, 2000; *Panning and Romanowicz*, 2006), we have developed the tools allowing us to invert both for radial and azimuthal anisotropy in the upper mantle, at the continental scale, using time-domain teleseismic long period fundamental and overtone wavepackets. Our results for a radially anisotropic tomographic inversion, based on data from available "pre-EarthScope" stations in North America (*Marone et al.*, 2006), confirm the well-known correlation with tectonics of 3D seismic velocity in the first 200 km under the North American continent (e.g. *Romanowicz*, 1979; *Alsina et al.*, 1996; *Van der Lee and Nolet*, 1997). In fact, a striking difference between the low velocity tectonically active western region and the high velocity stable central and eastern shields is observed, with a boundary almost perfectly coincident with the Rocky Mountain Front (Fig. 2). This pronounced contrast persists down to 200-250 km depth, where the 3D structure changes character, and the large velocity perturbations ($\delta \ln V_S > 4\%$) observed in the uppermost mantle make way to anomalies not exceeding 2-3%. High heat flow values (e.g. *Blackwell and Steele*, 1992) suggest that the imaged negative velocity perturbations in the western US represent young hot upper mantle material. East of the Rocky Mountain Front, our model, like others, shows a large area of fast isotropic V_S. This anomaly represents the lithospheric root of the North American craton. It extends to about 250 km depth in the oldest part of the continent. Other existing regional V_S models (e.g. *Van der Lee and Nolet*, 1997; *Frederiksen et al.*, 2001; *Van der Lee and Fredericksen*, 2005, *Nettles and Dziewonski*, 2004) show a similar feature. At 250 km depth, a low velocity anomaly is found beneath the Appalachians. This feature has been previously observed both in V_p (*Romanowicz*, 1979) and V_s (e.g. *Li et al.*, 2003; *Van der Lee and Fredericksen*, 2005) models. It may be due to intrusion of asthenosphere into the edge of the continental keel (*Li et al.*, 2003). Alternatively, this anomaly could be an indication of the presence of water in the mantle, dating back to the subduction of the Iapetus ocean or related to the subducted Farallon plate (*Van der Lee et al.*, 2005). Deeper than 250-300 km depth, the anomaly amplitudes significantly decrease throughout the continent and heterogeneities are reduced to less than +/-2%. The deep upper mantle is characterized by the presence of fast material beneath western North America, which we relate to subducted slabs: the Juan de Fuca plate in the north and the extinct Farallon plate in the south.

In terms of radially anisotropic structure, the shallow part of the North American upper mantle is

dominated by a positive δln ξ anomaly (where $\xi = [(Vsh-Vsv)/Vsv]^2$), suggesting preferential orientation of the fast axis of anisotropic mantle minerals in the horizontal plane (Fig. 2). For instance, at 100 km depth, a positive ξ anomaly is imaged both beneath the North American continent and the surrounding oceans. At this depth, the origin of this feature must be lithospheric under the continent, and asthenospheric in oceanic areas. Deeper, this widespread positive ξ anomaly disappears beneath the oceans and its presence is mainly restricted to the cratonic part of the North American continent (Fig. 2). At 250-300 km depth, asthenospheric conditions are present throughout the study region, as suggested by the isotropic Vs structure. Persisting radial anisotropy beneath large areas of North America suggests an asthenospheric origin for this feature. The positive sign of this anomaly is consistent with horizontal shear flow causing the preferred alignment of anisotropic minerals and confirms the results obtained under cratons at the global scale (e.g. *Gung et al*., 2003). The model also suggests the presence of $V_{SH} > V_{SV}$ in a region surrounding the stable keel, in agreement with the inferences of *Fouch et al*. (2000).

Our preliminary results for the distribution of azimuthal anisotropy under the North American continent (*Marone and Romanowicz*, 2005, 2006b) confirm this view: they reveal the presence of two distinct depth domains of anisotropy under the central and eastern part of the continent (Fig. 3), with different directions of the fast axis, roughly following the domains imaged with isotropic Vs and radial anisotropy. A direction sub-parallel to the absolute plate motion is obtained at shallow depths (~100 km) in the West, whereas it is closer to north-south in central and eastern North America, consistent with directions obtained from short period surface waves by *Li et al*. (2003) and from a narrow band analysis of shear wave splitting (*Yuan and Dueker*, 2006). Determining the tilt of the fast axis in our model is currently underway, as this information is available from the radial and azimuthal anisotropy maps (*Montagner and Nataf*, 1988).

Thus our results, combined with those of previous studies (e.g. *Levin et al*.,1999; *Li et al*., 2003; *Gaherty*, 2004) indicate the presence of two distinct anisotropy domains under North America, one, at shallower depth, most likely associated with the lithosphere, and the other, at greater depth, with the asthenosphere. These domains differ both in isotropic velocity and in the character of anisotropy. The boundary between these two domains, which we will refer to as the LAB, although not precisely mapped, varies laterally, following the surface tectonic and geological structure. More specific evidence for such depth variations has been recently found using Sp and Ps scattered waves, as will be described below.

Our tomography results do not support the view of the LAB being the bottom of an anisotropic upper mantle region (e.g. *Karato*, 1992; *Gaherty and Jordan*, 1995), but rather a boundary between two domains of different anisotropy. They also support a maximum LAB depth of about 200-250 km, consistent with other geophysical data (*Rudnick et al*., 1998; *Jaupart et al*., 1998; *Hirth et al*., 2000). This is also consistent with regional observations under the Australian shield (*Debayle and Kennett*, 2000; *Simons et al*., 2002; *Debayle et al*., 2005), and, albeit at shallower depths, under the Pacific basin, where *Smith et al*. (2004) also suggested the presence of two layers with distinct azimuthal anisotropy, at lithospheric and asthenospheric depths, respectively. The nature and extent of a "tectosphere" that would translate coherently with continental keels, a controversial notion that has been the subject of debate in the last 25 years (e.g. *Jordan*, 1975; *Anderson*, 1979), needs to be revisited in the light of these studies.

Mapping more precisely, at the continental scale, lateral variations in the depth of this LAB, as well as its relation to anisotropy will shed important light on lithosphere/asthenosphere dynamics as well as the compositional nature of the LAB under continents.

Mapping mantle discontinuities

Defining the location and properties of the LAB within the North American upper mantle is a key goal of the proposed work. A discontinuity associated with the LAB has not been observed in global stacks (e.g. *Shearer*, 1991), possibly because of its large variations in depth. However, relatively sharp velocity gradients have been observed in numerous regions around the globe using a variety of methods. Discontinuities associated with a transition from a fast seismic lid to a deeper, slower low-velocity zone have been observed by several reflection and refraction experiments (*MONA LISA Working Group*, 1997;

Morozova et al., 1999; *Ryberg et al*., 1996; *Steer et al*., 1998a; *Steer et al*., 1998b; *Thybo and Perchuc*, 1997). Regional imaging of discontinuities has also been obtained using reflected teleseismic body-wave phases (*Revenaugh and Jordan*, 1991; *Revenaugh and Sipkin*, 1994), and recently progress has been made using Ps and Sp scattered phases (*Bostock*, 1998; *Collins et al*., 2001; *Farra and Vinnik*, 2000; *Kumar et al*., 2005a; *Kumar et al*., 2005b; *Li et al*., 2000; *Li et al*., 2004; *Li et al*., 2006; *Oreshin et al*., 2002; *Ramesh et al*., 2002; *Rychert et al*., 2005; *Rychert et al*., 2006; *Wilson et al*., 2005b).

Sp phases have become a popular tool for imaging the LAB because Sp imaging avoids complications due to reverberations from shallower discontinuities that are present in Ps data. For example, Sp imaging has illuminated a velocity drop at the LAB beneath several continental regions over a wide range of depths, including a region spanning the Kazakh Shield, the Tien Shen orogenic belt, the Tarim Basin, and the Pamir and Karakoram orogenic belts where LAB depths vary from 90 to more than 200 km (*Kumar et al*., 2005b; *Oreshin et al*., 2002); a clear LAB has also been observed beneath the Tibetan Plateau to depths of 200 km (*Kumar et al*., 2006). Recently, Sp imaging in the western U.S. revealed a lithosphere-asthenosphere boundary at depths of 60-95 km (*Li et al*, 2006). However, Ps phases have been able to clearly image the LAB when reverberations from crustal structure do not interfere with direct phases from the LAB, for example in Hawaii (*Li et al*., 2000; *Li et al*., 2004), and in our own work in eastern North America (*Rychert et al*., 2005, 2006).

First with Ps phases (*Rychert et al*., 2005) and more recently with Sp phases (*Rychert et al*., 2006), we have identified a seismic velocity discontinuity (a velocity drop) at depths of 87-105 km (Fig. 4). Because this discontinuity is located within the depth range of the lithosphere to asthenosphere transition seen in surface wave tomography (*Van der Lee*, 2002; *Li et al*., 2003; *Marone et al*., 2006), we associate it with the LAB. A novel feature of our approach is that we invert the migrated waveforms for the absolute depth of the LAB and its velocity gradient using a damped least-squares method. Although parameter trade-off's exist between the velocity drop and the depth range over which it occurs, they may be reduced by jointly considering the complementary sensitivities of the Ps and Sp phases. At stations HRV and LMN, combined inversions of Sp and Ps data requires a strong, 5-10% velocity contrast that is also sharp, occurring over less than 11 km at depth. The magnitude of this velocity gradient is comparable to that seen in the surface wave tomography (*Van der Lee*, 2002; *Li et al*., 2003; *Marone et al*., 2006), but the maximum depth range over which it occurs is considerably smaller than the resolution limit of the surface wave inversions.

The sharpness and strength of this velocity gradient has important implications for its origin. In particular, it is too large to be explained by purely thermal gradients (*Rychert et al*., 2005, 2006). Using the relationship of shear-wave velocity to temperature developed by *Jackson et al*. (2002) based on experimental data, or the empirical relationship proposed by *Priestley and McKenzie* (2006), thermal gradients in excess of 15 °C $km^{-1}$are required to explain the observed velocity gradients. In numerical models of flow and thermal structure at the base of the continental lithosphere in which viscosity depends on temperature and pressure, but is not affected by composition, thermal gradients at the base of the lithosphere are typically less than 5 °C km^{-1}, and definitely less than 10 °C km^{-1} (*King and Ritsema*, 2000; *Zaranek et al*., 2004). Therefore, we conclude than another mechanism besides temperature is required to explain the observed velocity contrast. A boundary between a dry, depleted lithosphere and a hydrated, less depleted asthenosphere (e.g. *Hirth et al*., 2000) could create a very sharp discontinuity, although it is unclear whether the combined effects of depletion and hydration could produce a large enough drop in velocity (*Lee*, 2003; *Schutt and Lesher*, 2006; *Karato and Jung*, 1998). However, the observed velocity gradients could easily be explained by a small amount of melt in the asthenosphere (*Hammond and Humphreys*, 2000; *Kreutzmann et al*., 2004).

Extending the LAB velocity gradient analysis beneath the thicker cratonic lithosphere and combining it with the previously described anisotropic tomography models would shed light on whether a low velocity, highly strained, anisotropic asthenospheric layer is ubiquitous across the continent. The strength of the LAB velocity gradient would help to resolve the question of whether the sub-cratonic asthenosphere is enriched in volatiles, as suggested by conductivity data (*Hirth et al*., 2000). Observation of very strong velocity drops over small depth ranges would be diagnostic of melt below the LAB, a

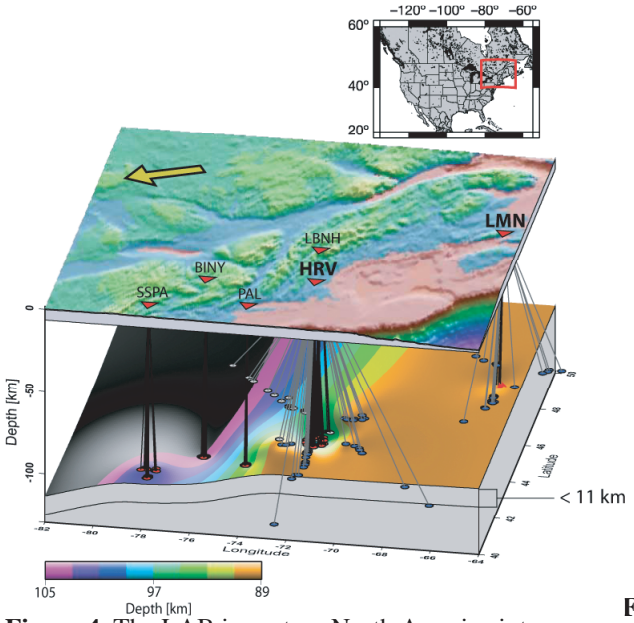

Figure 4. The LAB in eastern North America interpolated from migrated Ps and Sp waveforms (lower surface); red and blue circles mark Ps and Sp conversion points, respectively. Red triangles denote station locations. The Sp HRV data from northern back-azimuths and the Ps from LBNH (grey circles) are not used in the interpolation. All LAB depths were calculated assuming Vp/Vs=1.8 in the mantle.

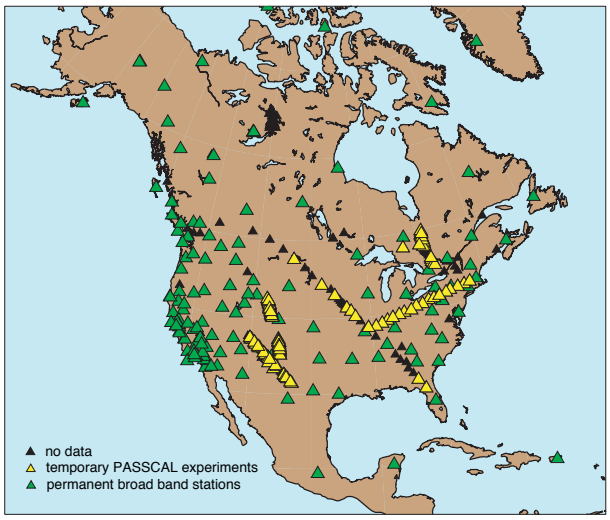

Figure 5. Broadband station distribution in North America as available for our recent tomographic study. Green: permanent broadband stations. Yellow: temporary PASSCAL deployments. Black triangles indicate stations for which surface wave data were either not available or not high enough quality to be used. In the proposed work, scattered wave phases will analyzed at permanent stations with a comparable distribution. Surface and scattered wave phases from EarthScope TA stations (not shown) will be incoporated in year 3 of the project.

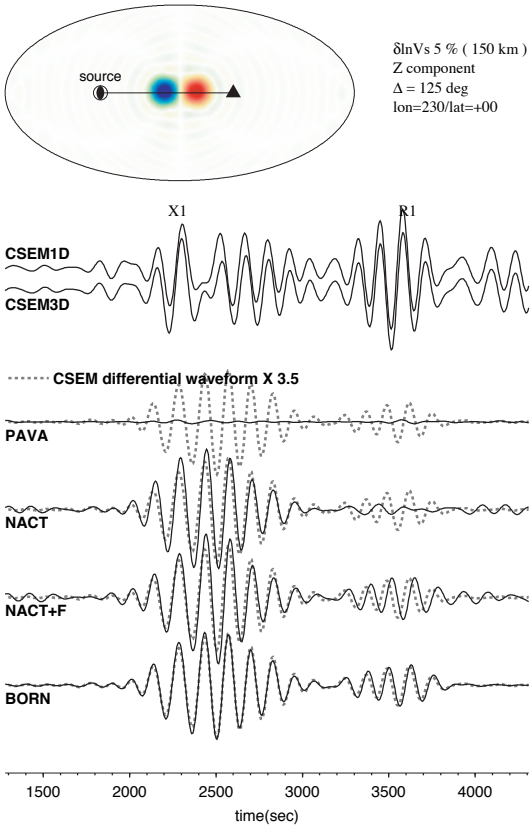

Figure 6. Comparison of vertical component synthetic seismograms for different normal mode-based approximations, computed down to 100 s period. The test model consists of 2 anomalies of strength δ lnVs = 5% and opposite sign centered at 150 km depth (50-250km) and of lateral extent ~800km. The reference "exact" seismograms (1D and 3D) were computed numerically using a coupled-SEM method (*Capdeville et al.*, 2003). Differential waveforms with respect to the 1D seismogram (continuous lines) are compared to the SEM differential seismograms (broken lines), for the Path Average surface wave Approximation (PAVA, 1D kernels), the NACT (2D kernels in the vertical plane), NACT plus out of plane focusing (NACT+F, 2.5D kernels) and finally the Born approximation. PAVA does not "see" the structure. The 2D sensitivity of the overtone packet (X1) is well captured by NACT, while adding focusing accounts for most of the out of plane perturbations in the fundamental mode (R1). What appears as a phase shift in the NACT+F differential trace is actually a small amplitude difference. The Born approximation gives a very good fit in this example, but is computationally much heavier.

finding which in turn would help to constrain the range of asthenospheric temperatures and compositions and, in the western U.S., processes related to recent magmatism.

Although the LAB is a primary focus of the proposed work, we also plan to investigate the implications of other discontinuities imaged by scattered waves for the North American tomography models. For example, discontinuities internal to the lithosphere have been observed (e.g. *Bostock*, 1998; *Levin and Park*, 2000; *Park and Levin*, 2001). Should such features occur over laterally extensive areas of North America, we will explore their incorporation into the tomography models. In addition, a variety of discontinuities in the mid-upper mantle have been detected within North America and globally, for example the discontinuity often called the Lehmann at depths of around 200 km. This discontinuity is sometimes seen preferentially under stable continents, sometimes not (e.g. *Anderson*, 1979; *Leven et al*., 1981; *Gu et al*., 2001; *Karato*, 1992; *Gaherty and Jordan*, 1995; *Deuss and Woodhouse*, 2002, *Vinnik et al*., 2005) and it has been suggested that it is the same as the LAB under continents (*Gung et al*., 2003). Discontinuities at somewhat greater depths have also been observed, for example the "X" discontinuity (e.g. *Dueker and Sheehan*, 1997; *Yuan et al*., 1997; *Owens et al*., 2000; *Sheehan et al*., 2000; *Li et al*., 2002; *Deuss and Woodhouse*, 2002; *Williams and Revenaugh*, 2005). We plan to explore how these mantle features relate to asthenospheric velocity gradients in the tomographic models. The mantle transition zone discontinuities at nominal depths of 410 and 660 km have been imaged across North America at a wide variety of scales (e.g. *Shearer*, 1991; *Bostock*, 1996; *Dueker and Sheehan*, 1997; *Li et al*., 1998; *Chevrot et al*., 1999; *Sheehan et al*., 2000; *Gu and Dziewonski*, 2002; *Gilbert et al*., 2003; *Fee and Dueker*, 2004; *Song et al*., 2004; *Wilson et al*., 2005b). Incorporation of an undulating 410 km discontinuity into the tomography models is a task proposed in the last year of the project.

Role of the proposed work in the context of EarthScope

Eventually, one of the goals of USArray deployments is to provide dense enough spatial sampling by broadband data in order to combine industry-style imaging techniques for reflectors and tomography to obtain high resolution maps of the main horizons in the North American crust and upper mantle. However, even with the 70 km station spacing of the Transportable Array, unaliased images of mantle interfaces using methods that involve forms of wave-field back propagation (e.g. *Bostock et al*., 2001; *Poppeliers and Pavlis*, 2003; *Levander*, 2003*; Levander et al*., 2006) will only be possible at depths greater than ~140 to 200 km *(Levander*, 2003; *Levander et al*., 2006; *Rondenay et al*., 2005). Because the LAB, which lies at considerably shallower depths in many regions of North America, is one of our primary targets, we adopt an approach which blends surface wave tomography with a modified form of one-dimensional migration.

We see our work as bridging the gap between current smooth, large scale tomographic modeling and the higher resolution modeling which is possible with the more densely spaced stations of Flexible Array experiments. One of our goals is to provide a good 3D reference or "backbone" model for such studies. In particular, the upper mantle velocity model that we propose to develop should contain sufficiently detailed information about lateral variations in volumetric heterogeneity and discontinuities that it will eventually help link the more detailed models of velocity structure enabled by Flexible Array deployments. For example, in the western U.S. where Transportable Array will become available over the three year duration of the proposed work, we anticipate a resolution of 200 km in lateral shear-wave velocity variations. Vertical resolution of LAB should be better than 5-10 km and lateral resolution of variations in LAB depth will be comparable to the station spacing. In addition, our model should provide new information on mantle density structure for geodynamical investigations, for example studies of the buoyancy of the continental lithosphere involving gravity data, and their implications for mantle depletion as a function of lithospheric age (e.g. *Perry et al*., 2003) or models of how the lithosphere interacts with asthenospheric flow (e.g. *Silver and Holt*, 2002; *Conrad and Lithgow-Bertelloni*, 2006; *Becker et al*., 2006; *Coblentz and Humphreys*, 2005).

Work Plan

Merging tomography and scattering horizon/receiver function methods can be viewed in a general framework of developing the tools to combine two complementary approaches for the investigation of 3D structure in the upper mantle – and also from the specific point of view of improving our understanding of the deep structure of the NAM continent. The proposed work includes a tool development part - combining the two approaches - and an application part, which will necessarily only gradually utilize new USArray data, as backbone stations come on line and as the TA marches across the continent. By the 3rd and last year of this proposal, we hope to be able to incorporate a sufficiently large number of high quality Earthscope data to start characterizing the depth continuation - or lack thereof, of the Rocky Mountain front, which is arguably the most striking "lateral" feature in tomographic models of NAM.

We note that large lateral variations in "volumetric" S velocity structure are present at the continental scale and throughout the upper-mantle, but that, at least at depths down to 250 km, these lateral variations seem to define the presence of large provinces of slowly varied properties separated by "boundaries" with sharp lateral or vertical gradients. This provides a framework for developing our joint inversion approach.

Waveform Tomography

We already have assembled a large dataset of long period (60-220 s) three component teleseismic waveforms for paths crossing the North American continent, recorded at permanent stations as well as several PASSCAL deployments across North America (MOMA, ABITIBI, FLED, CDROM, LARISTRA), from events at teleseismic as well as far regional distances ($15° < \Delta < 165°$), providing the best possible path and azimuthal coverage for the region (Fig. 5). Energy wavepackets corresponding to fundamental mode surface waves as well as overtones (X phase) are extracted automatically, selected by comparison with synthetic seismograms, and later visually inspected for quality, resulting in our current collection of over 18,000 fundamental mode and 20,000 overtone wavepackets. The separation of fundamental and overtone wavepackets allows us to assign different weights according to path redundancy and to enhance the contribution of higher modes in the inversion. We parametrize the 3D model in terms of B-splines in the vertical direction and spherical splines in the horizontal direction, with a tighter grid ("level 5" splines, corresponding to horizontal wavelengths of ~800 km) over North America. Waveforms are corrected for structure outside of the region of study using an existing degree-24 equivalent ("level 4" splines, ~1500km) radially anisotropic model (*Panning and Romanowicz*, 2006). Starting from solutions as provided in the Harvard CMT catalog (*Dziewonski et al*., 1981), we compute perturbations to the source parameters (location and moment tensor), performing path corrections in this global 3D model. Inside the region of study, the model is cast in terms of a set of 7 physical parameters, representing a transversely isotropic medium with arbitrary orientation of the fast axis (5 parameters: ACFLN and two angles, e.g. *Montagner and Nataf*, 1988). Inversion is first performed for radial anisotropy (only L and N are resolvable with the long period waveforms), then for azimuthal anisotropy, and finally the tilt of the axis of anisotropy can be retrieved. Modeling has been cast in the normal mode framework of the Non-linear Asymptotic Coupling theory (NACT, *Li and Romanowicz*, 1995), which includes across branch mode coupling and therefore allows 2D sensitivity kernels in the vertical plane, which is important for the inversion of overtone data (e.g. Fig. 6). Crustal corrections are performed using available crustal models (e.g Crust2.0) and a regionalization method which allows us to take into account more accurately non-linear effects due to the large lateral variations of Moho depth (*Marone and Romanowicz*, 2006a), which are not included in most conventional crustal corrections. In the future, we plan to incorporate constraints on crustal structure obtained from USArray data, for example Tom Owens' EarthScope Automated Receiver Survey (*Crotwell and Owens*, 2005).

So far, our modeling has not included focusing effects in the horizontal plane, i.e. sensitivity in the 3rd dimension (e.g. *Zhou et al*., 2005); however, we have developed the tools to include these, using either asymptotic expressions (*Romanowicz*, 1987; *Gung and Romanowicz*, 2004), which is fast but has limitations in applicability, or a more accurate, but more computationally expensive, non-linear Born

scheme (*Panning et al*., 2005, Fig. 6). Both of these tools are available for the present study. Several other modifications to our tomographic approach, regarding spatial and depth parametrization of the model, will be developed in the course of this study. In particular, we will investigate different ways to include the LAB and its lateral variations. We will also continue collecting high quality teleseismic waveform data, as new stations become operational and/or events occur in locations that fill holes in the current distribution.

Sp and Ps imaging

In the initial years of the project, Sp and Ps analysis will be focused on permanent broadband stations in North America, the stations of the EarthScope Backbone network in particular (Fig. 5). However, as our methods are developed, the Sp and Ps analysis will be expanded to the stations of the Transportable Array in year 3 of the project. Fischer is involved in a complementary project that also involves analysis of scattered phases at Transportable Array stations. For a discussion of personnel, please see the Brown Budget Justification.

The amplitudes of Ps and Sp phases are both primarily sensitive to shear-wave velocity contrast at a given discontinuity, but beyond that they have complementary strengths. Because Sp phases are free from crustal reverberations, they typically offer simpler waveforms and less ambiguous identification of the LAB. In Sp imaging it is necessary to avoid possible inference with unwanted phases such as SKS, pPPP, pPPPP, and sPPPP (*Wilson et al*., 2005a), but such interference can be minimized by avoiding certain sources, for example events from depths >300 km and epicentral distances greater than 80°. However, Ps phases do provide clear imaging of the LAB for a wide variety of regions. For example , at HRV a LAB Ps phase at ~97 km can be clearly distinguished from the reverberations of the 30 km thick crust (Fig. 7), although if the crust were a few kilometers thinner or the LAB ~10 km deeper, the reverberations would overprint the LAB phase. On the other hand, Ps phases typically have better signal-to-noise ratios at higher frequencies, and the higher the frequency of the incident wave, the tighter the vertical resolution of the scattering discontinuity. For example, the incident P waveform that corresponds to the migrated Ps phases observed at LMN (Fig. 8) has a dominant period of ~3 s, allowing gradients as sharp as 11 km to be resolved, whereas the migrated Sp phase is longer period (8 s) and has less sensitivity to gradient thickness (*Rychert et al*., 2005, 2006). We anticipate that Ps analysis of the LAB should be possible over broad regions of the continent, for example where crustal thicknesses are greater than 40 km and LAB depths less than 110 km, but Sp phases will likely be the more reliable detector in cratonic regions with the greatest lithospheric thicknesses. We also plan to incorporate other scattered teleseismic phases, such as SKSp which *Li et al*. (2006) found to be a very useful complement to Sp in their study of the LAB beneath the western US, and PKPs (Fig. 9).

Although scattered wave phases from the LAB in the western U.S. and the Appalachian province have been clearly observed (*Rychert et al*., 2005, 2006; *Li et al*., 2006), Sp and Ps phases beneath the thick cratonic lithosphere have not yet been systematically studied. However, other studies have found LAB phases at depths of 200 km and more (*Kumar et al*., 2005b; *Kumar et al*., 2006) including an early observation at 250 km depth beneath the Baltic Shield (*Sacks et al*., 1979). The presence or absence of a LAB phase beneath cratonic North America would be an important constraint on the LAB in the tomography models; an absence would indicate a fairly gradual velocity gradient (as opposed to poor detection) because permanent stations in the mid-continent have recorded abundant and well-distributed sources (Fig. 9). Ps phases are a proven tool for imaging deeper interfaces, such as the transition zone discontinuities (e.g. *Bostock*, 1996; *Dueker and Sheehan*, 1997; *Li et al*., 1998; *Chevrot et al*., 1999; *Sheehan et al*., 2000; *Gilbert et al*., 2003; *Fee and Dueker*, 2004; *Wilson et al*., 2005b). However, Sp phases also have produced useful constraints on transition zone structure (*Vinnik and Farra*, 2002; *Vinnik et al*., 2003) and we plan to explore their constraints beneath North America. Note that for deeper discontinuities, the most effective Sp epicentral distance ranges are more limited than for the LAB. The Sp data in Fig. 8 were tuned for LAB imaging, resulting in lower signal/noise ratios at transition zone depths.

The 70 km station spacing of the TA offers a potential increase in lateral resolution of discontinuity

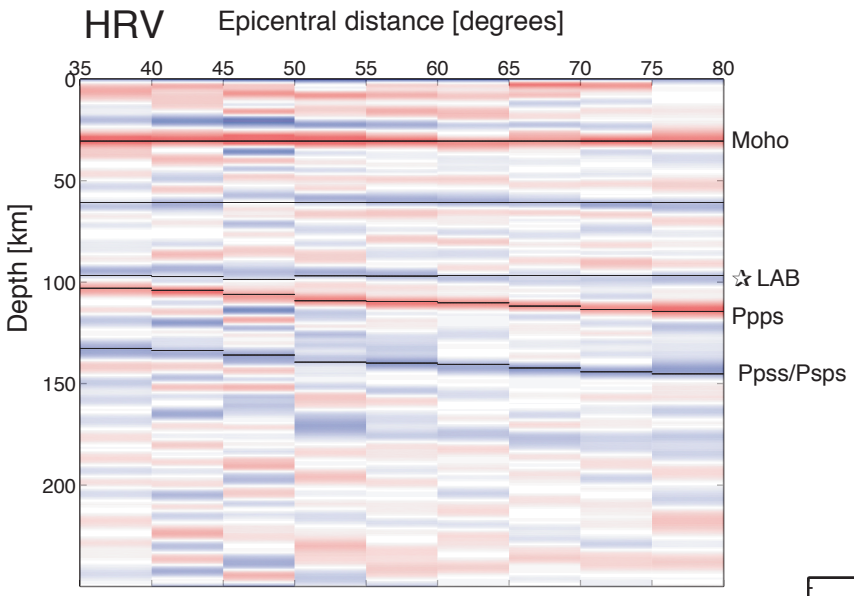

Figure 7. Ps waveforms from HRV deconvolved and migrated in epicentral distance bins. Red signifies positive polarity, or a velocity increase with depth, while blue indicates a negative amplitude corresponding to a velocity decrease with depth. Black lines indicate the migrated depths of synthetic phases predicted from our preferred HRV model, including direct conversions from the Moho (30 km), the LAB (97 km depth) and a possible interface at 61 km. Later arrivals show greater apparent depth with distance and correspond to crustal reverberations.

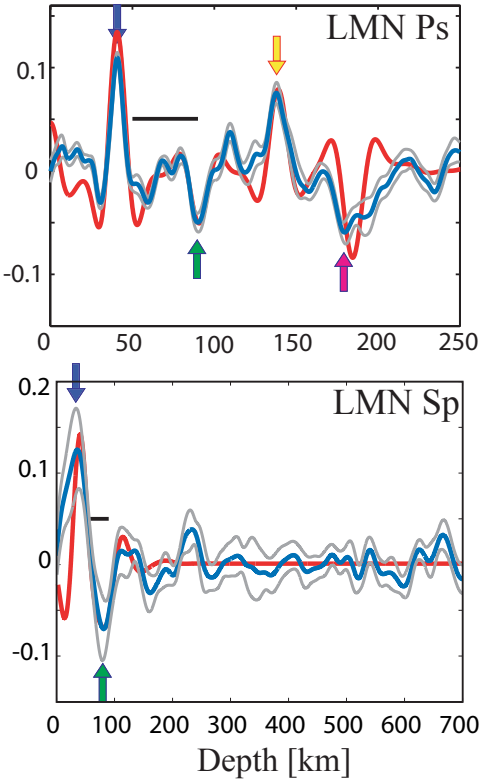

Figure 8. Ps and Sp waveforms migrated in a single bin at station LMN. A positive phase corresponds to a velocity increase with depth, while a negative phase indicates a velocity decrease with depth. Coloured arrows indicate phases from the base of the lithosphere (green), the Moho (dark blue), crustal reverberations (yellow and magenta). Error bars corresponding to two standard deviations (grey lines) were calculated with bootstrap tests. Red lines correspond to migrated synthetics from the best-fitting velocity model; while we model the LAB velocity gradient by matching the LAB waveform, for the Moho we model only depth and do not fit phase amplitudes. Black lines correspond to the greatest negative velocity gradient determined by surface wave models (*Li et al.* (2003), *Van der Lee* (2002)). Sp waveforms have been reversed in polarity and time for comparison with Ps. Ps and Sp indicate similar LAB properties: a 6.0-9.6% drop in shear-wave velocity over less than 11 km located at a depth of ~90 km.

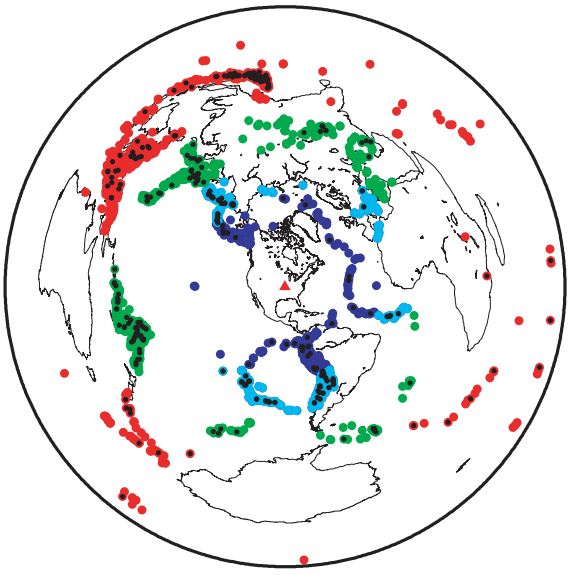

Figure 9. Distribution of sources around permanent broadband station CCM (Cathedral Caves, Missouri). Colors correspond to events from 1989 to 2005 in distance ranges appropriate for Ps (35°-80°, dark and light blue, 926 events), Sp (60°-80°, light blue, 520 events), SKSp (85°-110°, green, 893 events), and PKPs (120°-180°, red, 547 events). Events with mb > 5.7 are shown for Ps and Sp, and events with mb > 6.0 for PKPs and SKSp. Black dots are events in the last two years, and illustrate an event distribution that might be expected for a Transportable Array station.

structure. Given the 2 year recording interval of TA stations, obviously the number of paths to a given station will be more limited than with permanent stations. However, data at TA stations should be sufficient for at least Sp imaging. For example, we constructed a migrated Sp waveform for permanent station HRV using two years of data and found it be identical at 95% confidence to the migrated waveform for the complete dataset that spanned more than 14 years. In addition, Sp imaging of the LAB has been successfully carried out using roughly 2 year datasets from portable arrays in Tibet (*Kumar et al*., 2006), the Tien Shan (*Kumar et al.,* 2005b) and Iceland (*Kumar et al*., 2005a). Finally, the two-dimensional 70 km station spacing of TA will provide significant overlap of Sp and SKSp LAB conversion points between stations, and more limited overlap of Ps and PKPs LAB conversion points, at least partially compensating for the smaller number of events that will be recorded. In summary, Sp imaging of the LAB will very likely be successful using TA data. Ps imaging may be possible, particularly where the LAB phase is well-separated in time from crustal reverberations, and for deeper mantle discontinuities, such as the 410 and 660 km interfaces.

Constructing a 3D starting model

One of the critical tasks of this project will be to construct an appropriate 3D isotropic starting model based on the current tomographic results (volumetric heterogeneity) as well as information on depth to the LAB and its velocity contrast from the converted phase data. We will experiment with different parametrizations so as to accommodate the sharp LAB and its lateral variations.

To obtain constraints on the depth to the LAB and its velocity contrast from the Sp and Ps data for the new starting shear-wave velocity model, we can employ the approaches that we have already developed (*Rychert et al*., 2005, 2006), with some modification to account for information on three-dimensional shear-wave velocity heterogeneity provided by the existing tomography models *(Marone et al*., 2006).

Waveforms for a specific phase type (e.g. Ps and PKPs versus Sp and SKSp) will be binned according to the geographic position at which their paths intersect trial LAB depths (or in later work, the depths of deeper scattering interfaces). We plan to experiment with different binning schemes to optimize spatial resolution of discontinuity properties while assuring robust waveform migration. Where stations are closely enough spaced that scattering points overlap, data from different stations will be combined. This is most likely to be true for Sp phases; see for example the distribution of scattering points at eastern stations HRV and LMN from *Rychert et al*. (2006) (Fig. 4). However, in the actual joint inversion of scattered wave and long period waveform data described later, scattered wave data will be separated by station to retain as much path-specific information as possible. When using the binned, deconvolved and migrated scattered wave data to refine the tomography starting model, the ray-based scattering point positions in a given bin will be interpreted in light of their actual Fresnel zones which are on the order of 10's of kilometers for scattering depths of 100-200 km.

The waveforms will be decomposed into P and S components using a free-surface transformation matrix and then simultaneously deconvolved in the frequency domain and migrated to depth using the approach developed by *Bostock* (1998). However, in contrast to our previous studies, we will now introduce path-specific corrections for lateral heterogeneity by modifying the phase delay terms in the deconvolution and migration operator. This approach is equivalent to using a move-out correction for each phase which accounts for lateral heterogeneity. However, we also plan to experiment with other approaches to deconvolution, for example the multi-taper deconvolution approach of *Park and Levin* (2000). For Ps phases, we will deconvolve P from SV and SH components, and for Sp, SV and SH from P. The starting model we are constructing at this stage is isotropic, and the ability to image the LAB and other discontinuities will in general rely on the higher signal-to-noise deconvolutions involving SV. However, when robust signals appear with SH deconvolutions, they offer complementary resolution of anisotropy and dipping interfaces.

To determine approximate, initial constraints on the velocity gradient at the LAB as well as LAB depth, we will invert the migrated waveforms for the absolute depth of the LAB gradient, the magnitude of the shear-wave velocity drop and the depth range over which it occurs using a damped least-squares method (*Rychert et al*., 2005; *Rychert et al*., 2006). The scattered waveforms also depend on the period

of the incident wave, but this parameter may be constrained independently by modeling the direct P waveform (for Ps) or the direct S waveform (for Sp). Trade-offs between the absolute depth, depth extent, and magnitude of the LAB velocity gradient will be carefully assessed, as will the effects of shallower discontinuities such as the Moho. To accurately calculate predicted migrated waveform amplitudes and the partial derivatives of the predicted migrated waveform with respect to discontinuity parameters, propagator matrix synthetic seismograms will be generated for the incident wave slowness of each of the real waveforms, the synthetics will be scaled to the amplitudes of their noise-normalized, real waveform counterparts, and identical deconvolution regularizations will be applied. This procedure will ensure that we accurately accounted for differences in phase amplitude produced by waveforms with varying incidence angle.

Joint inversion of long period waveforms and scattered waves

The starting 3D model will then be used in a joint inversion of long period waveforms and scattered waves. This involves a forward modelling part. Accurate crustal corrections will be applied, as previously described, to the long period data. We will need to determine whether the lateral variations in the LAB and the corresponding lateral velocity contrasts are within the acceptable range of normal mode first order perturbation theory and whether we can "get away" with using an average 1D LAB model for the entire continent to compute normal mode sensitivity kernels. This will be the initial approach, but we can later incorporate laterally varying (regionalized) reference eigenfunctions, or simply move to the computation of synthetic seismograms using a large scale regional SEM code (with spherical geometry) under development (*Romanowicz et al*., 2006).

The joint inversion will be set up iteratively. We will first refine the tomographic model, including isotropic S velocity structure down to 660 km as well as radial and azimuthal anisotropy which we will allow to a maximum depth to be determined (including constraints from SKS splitting, as previously), subject to the constraints on the velocity contrast across the LAB from the converted phase data. In the next iteration, the depth to the LAB and velocity gradient across the LAB will be refined, and then back to the tomographic model. This will necessitate an adequate parametrization of the model. Beyond the spherical splines (horizontal direction, *Wang and Dahlen* 1995) and B-splines (vertical direction) which we currently use, we plan to experiment with other multiscale wavelet (e.g. *Daubechies*, 1992), and, if appropriate, curvelet decompositions (curvelets are a generalization of wavelets; e.g. *Candès and Guo*, 2002; *Candès and Donoho*, 2004) that can accommodate strong gradients across boundaries between large domains of smoothly varying structure (e.g. LAB, Rocky mountain front). Another approach we will consider is a continuous parametrization with the specification of correlation lengths in the framework of generalized inversion theory (e.g. *Tarantola and Valette*, 1982; *Montagner and Jobert*, 1988).

To prepare the Ps and Sp data for the joint inversion, the waveforms will be re-migrated using the refined 3D model described in the previous paragraph. We propose to carry out the joint inversions in two stages. In the first stage, we will focus on constraining LAB depth using LAB phase travel-times. The depth of the LAB phase apparent on the migrated waveforms for each bin will be converted to the equivalent travel-time (plus uncertainties) for each path contributing to the bin. Scattered wave travel-times and partial derivatives with respect to discontinuity depth will be predicted by ray-tracing through the 3D model. After each iteration, the scattered wave data will be re-migrated to account for changes in the 3D model. Because we are solving for shear-wave structure and Ps and Sp times are also affected by Vp/Vs, we will need to assess the effect of Vp/Vs ratios on the inversions. Even for extreme variations in mantle Vp/Vs (for example a variation of 1.7 to 1.8, the maximum range seen in mantle xenoliths (*Lee*, 2003)) LAB depths at ~100 km determined individually from Ps or Sp vary by less than 8 km (*Rychert et al*., 2006). Nonetheless, we will experiment with fixing mantle Vp/Vs at different values that are uniform throughout the mantle or in large model sub-regions, and also with using the travel-times of direct teleseismic S and P phases to provide independent constraints on Vp/Vs (e.g. *Niu et al*., 2004).

In the second stage, the amplitude and shape of the LAB waveform for each bin will be added as constraints on the LAB velocity gradient. The predicted waveforms and partial derivatives will in this

case be calculated using propagator matrix synthetics from 1D structures that locally represent the portion of the 3D model sampled by the data in a given bin. Because our propagator matrix code is implemented for anisotropic elastic coefficients with an arbitrary orientation, this same synthetic approach can be employed for inversions in anisotropic models. The scattered wave data may lack the ability to resolve anisotropy in the strength of the discontinuity, but with the anisotropic propagator matrix synthetics we can assure that the effects of anisotropy implied by the surface wave data are accounted for in the treatment of the scattered phases.

Further steps

Once the lithosphere-asthenosphere part of the model is stable, we will shift our attention to the deeper features and discontinuities in the upper mantle. We anticipate that the scattered phase data, corrected for volumetric structure, will show clearer signatures of the 410 km and 660 km discontinuities, and possibly will allow us to determine whether a ~200 km discontinuity (i.e. the Lehmann) exists even in areas where the LAB is much shallower. We will also assess the existence and implications of other discontinuities such as the "X", and look for evidence for the base of the asthenosphere in the tomographic model obtained. At this point, we will augment our tomographic waveform dataset with teleseismic body waveforms, and in particular SS waveforms that have bouncing points under the region of study. Such waveforms can be readily incorporated in our tomographic formalism (down to 16 sec period), just as we do it at the global scale (e.g. *Mégnin and Romanowicz*, 2000) and can be corrected for structure outside of the region using an existing global model (e.g. *Panning and Romanowicz*, 2006 – other models will also be tested).

As the TA progresses and the backbone network's holes are filled, we will be in a position to incorporate regional distance long period waveforms across the continent, for a small number (10-15) of high quality events; using broadband numerical synthetics (regional SEM) we will assess where our 3D model requires adjustments.

Throughout the project, we plan to actively seek out interdisciplinary interactions that will further our ability to interpret the developing velocity model. Here we describe a few potential examples, although numerous other possibilities also exist. 1) The proposed work will result in sharper resolution of the LAB and of layering of anisotropy above and below it, and we look forward to working with geodynamicists and mineral physicists to better understand the implications of these findings for mantle flow, lithosphere-asthenosphere dynamics, and the physical and chemical properties that differentiate the lithosphere from the asthenosphere. 2) When combined with gravity data, our model will offer new constraints on upper mantle density structure, and, potentially, how competing buoyancy effects due to chemical depletion and temperature vary as a function of lithospheric age (e.g. *Perry et al*., 2003). 3) Our model may manifest strong variations in LAB depth, LAB velocity gradients and volumetric heterogeneity between major tectonic provinces. In such a case we would work with other investigators to integrate these findings with xenolith data, surface geology, geodetic data and regional tectonic models.

Dissemination of Results

In addition to publishing our results in journals and presenting them at meetings, we also plan to make our upper mantle velocity models openly available through the Searchable Product Archive and Discovery Engine (SPADE) currently being developed by Tim Ahern and the IRIS DMC. The SPADE will provide a coherent web services-based system to manage submission, archiving, query, and access of USArray and other EarthScope data and information products.

Project Timeline

Year 1:

Brown: Analyze scattered waves at permanent broadband stations across the continental US. Determine depth of LAB and other lithospheric discontinuities wherever detected, as well as velocity jump across LAB, correcting for existing 3D isotropic velocity structure.

UCB: Development of suitable 3D model parametrization to accommodate strong gradients across LAB

and test of theoretical approximations for forward modeling. Initial 3D model construction based on available scattered phase data and testing.

***Year 2*:**
UCB: Compute synthetic long period waveforms for starting model, including non-linear crustal corrections. Set up procedure for iterative inversion and implement.
Experiment with parametrizations that enable anisotropy to be confined to different domains (such as above and below the LAB). Start collecting body waveform data (some already available from global database).
Brown: Continue collecting and measuring scattered phases, and contribute code for incorporating scattered wave time and waveform information into iterative inversion. As iterations of inversion proceed, refine information on LAB velocity gradient and other lithospheric discontinuities.
Year 3:
UCB: Development of final 3D model with focus on resolving structure below the LAB, incorporating body waveform data.
Brown: Investigate deeper horizons (base of asthenosphere, 410 km discontinuity). Start incorporating data from TA. Test iterations and final model against scattered wave data.
All: Contribute model to SPADE.

Broader Impacts of the Proposed Work

The upper mantle velocity models we propose would provide continental-scale context for other researchers who are planning or interpreting more local seismological studies, including Flexible Array experiments. Our models would also be directly relevant to a wide range of geological, tectonic, and geodynamical investigations involving the North American lithosphere, asthenosphere and transition zone. In addition, the proposed work would contribute to the training of a post-doc and graduate students at Berkeley and Brown.

Results from Prior NSF support

B. Romanowicz, NSF EAR-0345481: $124,047, 03/01/04-02/28/07, "*Towards Characterizing Depth and Lateral Variations of Anisotropy Across the North American Continent*". This grant has supported the development and implementation of the formalism for inverting three-component long period seismograms for 3D isotropic and both radial and azimuthal anisotropy in the upper mantle as well as including constraints from SKS splitting measurements. In the process, we have also developed a non-linear methodology to deal with crustal corrections. *Publications*: *Marone and Romanowicz* (2006a,b); *Marone et al*. (2006). *Marone and Romanowicz* (in prep, 2006). *Broader impacts*: This award contributed to the education of one post-doc (F. Marone).
K. M. Fischer, NSF EAR-0208284: $236,825, 7/1/02-6/31/06, "*Migration imaging of mid-upper mantle discontinuities*". Results from the award include the Ps and Sp imaging of the lithosphere-asthenosphere boundary beneath eastern North America described in this proposal. In a third study, comparison of shear-wave splitting in regional S phases and teleseismic SKS phases at stations in the western Himalayan syntaxis demonstrates that much of the SKS splitting is due to anisotropy at depths below the lithosphere and is consistent with shear or extension in the asthenosphere parallel to the overall trend of the orogen. *Broader impacts*: This award contributed to the education of three graduate students (Catherine Rychert, Christine McCarthy and Dayanthie Weeraratne) and a post-doc (Stéphane Rondenay). *Publications*: *Rychert et al*. (2005); *Rychert et al*. (2006); *Weeraratne et al*.(in prep., 2006).